Available online at www.sciencedirect.com

ScienceDirect

Ceramics International 40 (2014) 4407–4414

CERAMICS INTERNATIONAL

www.elsevier.com/locate/ceramint

Significant improvement of refractoriness of Al_2O_3–C castables containing calcium aluminate nano-coatings on graphite

S. Dutta, P. Das, A. Das, S. Mukhopadhyay*

Department of Chemical Technology (Ceramic Engineering Division), University of Calcutta, 92 APC Road, Kolkata 700009, India

Received 1 August 2013; received in revised form 26 August 2013; accepted 26 August 2013
Available online 5 September 2013

Abstract

The performance of alumina-carbon castables containing graphite flakes coated by nanosized Ca-doped γ-Al_2O_3 phases has been investigated in terms of refractoriness under load (RUL) and oxidation resistance tests. The coating characteristics and its beneficial effects in castable matrix have been conceived by water-wettability test, differential scanning calorimetry and some physical characteristics. In this regard, a schematic representation of coated graphite has been proposed to elucidate its sustainability in the refractory mass. The comparative gain in performance of the refractory has also been ascertained by scanning electron microscope (SEM) and X-ray diffraction (XRD) studies of the castable matrix. The sol–gel coating overcomes the pitfalls of including uncoated graphites in castables and should be explored for commercial utilization.

Keywords: B. X-ray methods; D. Al_2O_3, Carbon; E. Refractories; Nano-coatings

1. Introduction

The fast pace of technological advancement has urged for the demand of more robust and stringent property specifications for refractories and monoliths. It provides longer campaign life in ladles, converters, blast furnace hearth, incinerators, boilers, rotary kiln sintering zone, etc. Various castable systems e.g. Al_2O_3, SiO_2, MgO, Al_2O_3–MgO, Al_2O_3–SiC, Al_2O_3–$MgAl_2O_4$ etc have gained popularity but carbon containing and nano-bonded castables are the latest substitutes for both ferrous and non-ferrous industries [1,2].

Carbon in the form of natural graphite or from pitch, resin, carbon black and coke can be present to the extent of 4–30 wt% in castable and refractory systems. Incorporation of carbon in the form of liquid binders like tar, resin and pitch has been known since decades [3]. But due to liberation of hazardous pyrolysis products, choice of solid form of carbon is nowadays more intended. Graphites are, however, much appreciated owing to their chemical, mechanical, thermal stability and other appreciable characteristics. Flaky graphite possesses some drawbacks if its content is increased. Increase in carbon content leads to risk of higher carbon pick up from castable affecting the quality of steel. Also chances of deformation of steel vessel exist due to increased shell temperature as a result of higher thermal conductivity of carbon [4]. Thus to reduce the energy consumption per unit of steel produced, an optimum carbon content is to be selected.

Though graphite offers several advantages to the castable matrix, its main limitations are low water-wettability and poor oxidation resistance. The main challenge is to disperse flaky graphite in a water-based castable batch with minimum casting water so as to obtain a dense structure after firing. A secondary problem of atmospheric pollution arises due to emission of carbon monoxide (CO) and/or carbon dioxide (CO_2) gases because of prevailing oxidizing atmosphere at the application site. Surface modification of graphite has thus been adopted by many researchers with a desire to reduce water content of batch and minimize rate of emission of carbonaceous products by environmentally benign manner [5–7]. The use of novel forms of carbon materials e.g. carbon nanotubes, graphene platelets and nanosheets in refractory ceramics recently opened up newer possibilities for carbon containing refractories [8–13].

Various scientists have tried to modify the surface with different types of coatings though each one has its own distinct merits and demerits [14–16]. Sol–gel methods, in this regard,

*Corresponding author. Tel.: +91 033 2350 8386; fax: +91 033 2351 9755.
E-mail address: msunanda_cct@yahoo.co.in (S. Mukhopadhyay).

0272-8842/$ - see front matter © 2013 Elsevier Ltd and Techna Group S.r.l. All rights reserved.
http://dx.doi.org/10.1016/j.ceramint.2013.08.112

had been and are still being practiced, stemming from its operational simplicity, moderate reaction parameters and reproducible coating quality. However, only a handful of reports are available that takes the full advantage of this method [17–19].

In spite of cost factor, sol–gel based coatings with binary oxides has been dealt with by some researchers. Selective thin coating, prepared by a hybrid set of precursors and applied over flaky graphite can make a balance between cost factor and coating quality [20,21]. In other words, an optimization between utilization of inherent graphitic properties as well as a stronger linkage of graphite with composite matrix can be realized.

Calcium aluminate based coatings, in this context, needs further exploration. Calcium aluminate cement, a crucial hydraulic material to bind aggregate and matrix in conventional, low and ultra-low cement castables has its own merits. Development of calcium aluminate forming bond over the hydrophobic graphitic surface has been investigated in detail in our previous publications [22,23]. The nanostructured Ca-doped γ-Al_2O_3 phases possessing Lewis acidic characteristics are sporadically distributed over graphite flake thereby improving its hydrophilicity. Heat treatment of this graphite under oxidizing conditions (at controlled pH) leads to development of some graphite oxide regions containing hydrophilic functional groups like carboxylic (–COOH), hydroxyl (–OH) etc. Zeta-potential test confirmed that it rendered better miscibility of castable matrix fines with minimum quantity of water. Raman spectroscopy studies revealed that partial exfoliation of graphite helped in the development of sp^2 hybridized small sheets of graphene-like regions [24]. These were responsible for better intercalation of Ca-ions and boehmitic nano-crystallites in between the sheets. It provided better connectivity of hydrophilic Lewis acidic sites with the adjacent aromatic ring structure via the functional groups present on surfaces and edges. The nanostructured phases of Ca-doped γ-Al_2O_3 also improved the surface area and intimately bonded the graphene sheets through the defects, fine pores and cleavages present. As a result graphite is well retained within the alumina based castable batch via better bonding of the matrix with the coating constituents.

Flaky graphites (both coated and uncoated) to the extent of 5.0% has been incorporated in a high alumina castable batch in this work. A comparison between the physical properties, thermal shock resistance and slag resistance of above mentioned castables had already been reported in our last papers [7,22–24]. However it is worth discussing the other refractory characteristics in detail to extrapolate the possibility of including increasing amount of coated graphites in refractories. The present investigation entails the mechanism of dramatic improvement of refractoriness, e.g. RUL and oxidation resistance by incorporation of only 5.0% of coated graphite. The matrix part of monolithic mass containing the surface-modified graphite has been separately characterized. The role of partially formed cross-linked nanoplatelets of graphite oxide in the refractory matrix, in this context, has been emphasized. In addition, the coating characteristics and phase evolution in castable have also been studied in depth to substantiate the refractory performance.

2. Experimental

Refractory grade natural flaky graphite having 97% fixed carbon and surface area 1.82 m^2/gm has been selected for this investigation. The sol–gel synthesis of calcium aluminate and preparation of that coating on graphite flakes had been discussed elsewhere in detail [22,23]. Stoichiometric calcium nitrate and aluminum-sec-butoxide were the chief ingredients to prepare calcium aluminate precursor. Thermal analysis study of graphite has always been considered as an important parameter, especially for its refractory applications [25]. To allow a quantitative measure of the enthalpy changes as a function of temperature, differential scanning calorimetry (DSC) test of coated and uncoated graphites have been conducted. This experiment was carried out up to 1600 °C from room temperature with a heating rate of 10 K/min (in air), using a NETZSCH instrument (Model Jupiter F3). Water-wettability of as-received and calcium aluminate-coated graphites has been compared by a method reported by Yoshimatsu et al. [26]. The quantity of floated graphites at the water surface and sediment volume of at the bottom was qualitatively estimated by taking photo snaps.

The main objective of the present work is to retain graphite in the castable matrix for a longer duration at elevated temperatures. In this regard, an investigation on the probable mechanism of bonding of graphite in castable matrix was attempted. A pictorial representation of nanosized calcium-doped gamma alumina coatings on graphite platelets has therefore been proposed. This schematic model has been utilized later to explain the outstanding performance of the castable containing this graphite.

The effects of incorporation of 5.0 mass% of coated and uncoated graphite separately to a low cement (4.0%) high alumina castable had been studied in this work. The composition of refractory batches and preparation of castable cubes (25.4 mm^3) and cylinders (50 mm diam, 50 mm height) had been the same as published in our previous contributions [7,22–24]. White fused alumina particles (72.0%) in several fractions comprised of the aggregate part of the castable. Apart from graphite and cement fines, the matrix part included aluminum powder (0.5%), microfine alumina (10.0%), microsilica (0.5%) and 8.0% commercial alumina-rich preformed $MgAl_2O_4$ spinel fines (with Al_2O_3=78%). C+ and C− codes were used as usual for castables containing respectively coated and uncoated graphites. All such samples were cured at humid condition (24 h), followed by air drying (24 h) and oven drying at 110 °C (72 h). The dried castables were then heat-treated at 900 °C, 1200 °C, and 1500 °C with 2 h of soaking at each temperature.

The present contribution focuses mainly on two important properties of castables which had not been reported before. These are refractoriness under load (RUL) and oxidation resistance tests compared between C+ and C− castables. Apparent porosity (AP), cold crushing strength (CCS), bulk density (BD) and XRD reports had also been furnished as supporting information. XRD phase analysis of the C+ castable samples heat-treated at 110 °C and 1200 °C were performed using a PANalytical (XPERT-PRO) Instrument with Ni-filtrated CuKα radiation at 40 kV/20 mA. The AP, BD and CCS of all

the castables at 110, 900, 1200, and 1500 °C were determined according to ASTM C133-94, C133-97 and C 20-00 specifications. For this characterization, an average result of 4 samples was utilized at each temperature. The matrix part of monolithic refractories always played a crucial role in determining their high temperature performances. As such the matrix portion containing coated graphite has been dealt further in harsh condition. The matrix part of (C+) castable had been separately cast taking proportionate amount from the original batch as outlined in our last work [24]. The constituents incorporated to the composite matrix were high alumina cement (14.3%), preformed spinel (28.6%), coated graphite (17.8%), micronized alumina (35.7%), microsilica (1.8%) and aluminum powder (1.8%). It was heat-treated at 1500 °C/2 h and an in depth microstructural analysis (XRD and SEM) had been conducted. The RUL property of cylindrical pre-fired samples had been evaluated by applying a load (2 kg/cm^2) with a heating rate of 8 °C/min. The deformation behavior was specifically compared beyond 1000 °C by observing percent elongation and failure pattern. The oxidation resistance test of castables had been done inside covered alumina crucibles. Samples were kept within carbon beds prepared inside those crucibles and fired at 1400 °C/3 h [8,27]. The photographs highlighting the carbon-containing regions were taken to understand graphite retention along length and cross-section of those castables after the oxidation test.

3. Results and discussion

The DSC plots of coated and uncoated graphites (Fig. 1a) up to 1200 °C conspicuously show the advantageous effect of coating on graphite. In DSC the equipment is designed to allow a quantitative measure of enthalpy change as a function of either temperature (or time). In coated graphite control of graphite oxidation is obvious due to the sol–gel selective calcium aluminate nanocoating formation over graphite. Although both of them show high exothermic peaks from 650 °C to 1100 °C the peak maxima are respectively at 931 °C and 1040 °C for coated and uncoated graphites. The sol–gel coating therefore inhibits contact between atmospheric oxygen and graphite to lower down the enthalpy change in case of uncoated graphite. It also reveals that the activation energy needed for oxidation is lower in coated graphite; it could be due to evolution of reactive nanosheets of exfoliated graphene oxides after sol–gel treatment and calcination [13,24]. It has been reported that calcium doped gamma–alumina via sol–gel route progressively crystallizes to calcium aluminate at around 930 °C [22,23]. The peak at lower temperature region (around 350 °C) can be due to a lot of reasons. Sporadic graphite oxide formation at acidic pH and more crystallization of left over calcium doped gamma–alumina can be one reason. Secondly more defect sites formation and consequent chemisorption (with subsequent desorption) due to sol–gel coating can be the other reason for evolution of this small peak [25]. The photograph of the suspended graphite particles in water has been represented by Fig. 1b. It is confirmed that surface-treatment had a noticeable effect on water-wettability. Only a

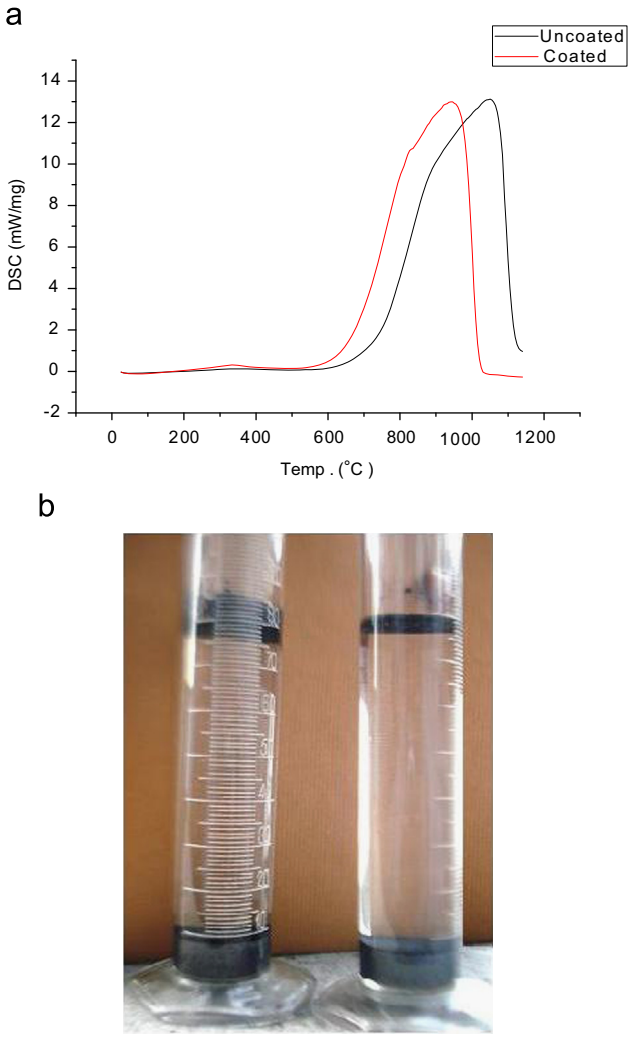

Fig. 1. (a) Differential scanning calorimetry studies of coated and uncoated graphites; (b) Water-wettability photos of coated and uncoated graphites (left—uncoated, right—coated).

thin layer of non-wetted graphite particles is observed while the bulk amount was completely immersed under water. As-received graphites, owing to their poor water-wettability, formed a much thicker black layer floating over the top surface of water. Dried and fired properties of (C+) and (C−) castables can be clearly distinguished due to this fundamental difference in hydrophilic behavior of two types of graphites.

The physical characteristics and spalling resistance of castables are discussed in our previous contribution [7]. Comparison of AP and CCS plots of C+ and C− castables from 110 °C to 1500 °C again confirms that the former possesses much better physical characteristics (Fig. 2). The batch contained 4.0% of cement (i.e. low cement type), however a huge amount of casting water (10.8%) was required for (C−) castable resembling a conventional castable. Although the mineralogical and chemical compositions are the same in C+ and C−, significant changes in physical properties were thus obvious between these two in relation to firing temperatures. The casting water requirement for C+ was found to be reasonably low (7.5%) compared to C− batch (10.8%) [22,23]. The hydrophilicity of coated graphite helped to

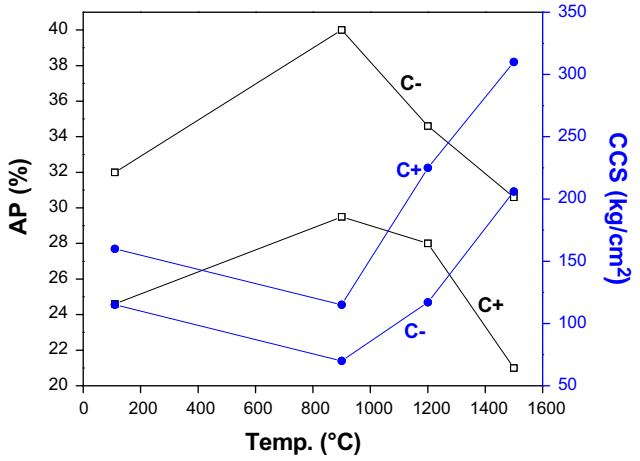

Fig. 2. Comparison of changes in apparent porosity (AP) and cold crushing strength (CCS) between C+ and C− castables with increasing temperatures.

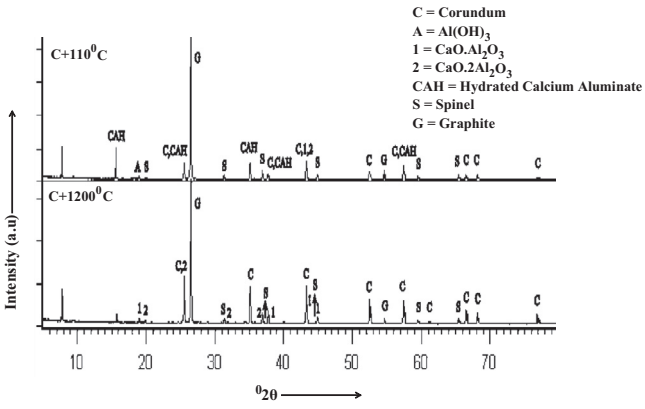

Fig. 3. XRD plots of C+ castable dried at 110 °C and fired at 1200 °C.

consume less water in C+ to attain proper consistency; consequently the apparent porosity and cold crushing strength at 900 °C are remarkably improved in the same. During hydration of cement CAH_{10}, C_2AH_8, C_3AH_6 and AH_3 phases (C = CaO, A = Al_2O_3, and H = H_2O) are generated in castable. On heating beyond 900 °C these hydrated compounds convert to CA, CA_2 etc., after complete dewatering. The bulk densities in C− varied from 2.52, 2.45, 2.54 g/cc respectively at 110 °C, intermediate and 1500 °C; whereas C+ showed 2.83, 2.72, 2.88 g/cc which are definitely much improved.

Fig. 3 represents the XRD plots C+ castable dried at 110 °C and fired at 1200 °C. The hydrated cementitious phases in castable are very much prominent at 110 °C. The other important phases are graphite and spinel taken in the matrix part. Alumina-rich preformed $MgAl_2O_4$ spinel fines (Al_2O_3 ~78%) used in this work are obtained commercially by very high thermal treatment (e.g. sintering at ~1900 °C) after some careful and lengthy steps of production namely, precalcination, cogrinding, drying and granulation. For obvious reason, their crystallinity remain unaltered at 110 °C and at higher temperatures. Peaks for corundum as well as hydrated alumina have also been identified from the plot due to the presence of alumina based aggregates and reactive alumina fines present in the matrix. After heat treatment at 1200 °C the hydrated cementitious phases are converted to calcium aluminate and calcium dialuminate after complete dewatering. The graphite peaks at around 27° and 55° are present in the plot even at 1200 °C; it once more substantiates that graphite is compatible to the oxidizing atmosphere due to the selective thin calcium aluminate coating over it. The C− castable, on the other hand, showed a significant loss in graphite after being fired at 1200 °C [7].

A simple schematic configuration of coated graphites has been intended in this contribution to explain the striking performance of C+ castables. Planar spacing in graphite structure is 3.4 Å which is much larger than Al^{3+} (0.58 Å), O^{2-} (1.24 Å) and Ca^{2+} (1.06 Å) ions. Ultrasonic treatment, as reported in literature, leads to exfoliation of graphite and dilation along *C*-axis [28]. Guest molecules can therefore be pushed into the graphite platelets to form intercalated compounds at particular temperature and pressure [29,30]. Literature shows that swelling of carbon bricks by intercalation compounds is observed in the hearth of blast furnace [3]. A similar mechanism of intercalation has been proposed in present work. Calcium-doped gamma alumina is the intermediate nanostructured phase of the sol–gel coating, possessing Lewis acid sites. The schematic diagram of the growing moiety of boehmite-derived hydrophilic γ-Al_2O_3 attached to graphite sheets is shown in Fig. 4(a) and (b). The nanostructured Ca-doped γ-Al_2O_3 crystallites tend to intercalate amongst the graphite platelets and envelops the graphite flakes. As a consequence, hydrophilicity of coated graphite increased as shown before; the prevailing oxidizing condition of coating synthesis also gives rise to some intermittent graphite oxide regions [22–24]. The octahedral sublattice in Fig. 4b represents less well-defined and poorly crystallized regions of boehmitic intermediate of γ-Al_2O_3 [31]. Octahedral sites of the moiety are occupied by Al^{3+} ions, whereas divalent cationic sites correspond to tetrahedral sites of defective spinel structure [32]. It is also opined that internal diffusion of Ca^{2+} takes place at ~600 °C up to a certain solubility limit. With due course of calcination (600 °C) the coating sporadically forms doped gamma alumina crystallites. The bridging mechanism of exfoliated graphite platelets via intercalated Ca-doped γ-Al_2O_3 nanophases has been proposed in Fig. 4**a**. Similar representation has been reported too by some other researchers [33]. After dehydroxylation of boehmitic γ-Al_2O_3 (doped) phases, a lot of defect sites are induced that are apportioned between octahedral and tetrahedral sites [34]. The aggregated nanophases containing these defect-enriched islands exchange and hold the ionic species with partially formed graphite oxide [19]. We suggest the coated graphite platelets are intermittently cross-linked with Ca^{2+} and Al^{3+} ions as shown in Fig. 4a; this arrangement should remarkably increase mechanical stiffness and strength of (C+) castable containing that exfoliated graphite [35]. Uncoated graphite, lacking such features, cannot help to improve the performance of (C−) castables. However, such schematic diagram needs experimental validation which is discussed later, especially by the noticeable increase in RUL property of the respective castable.

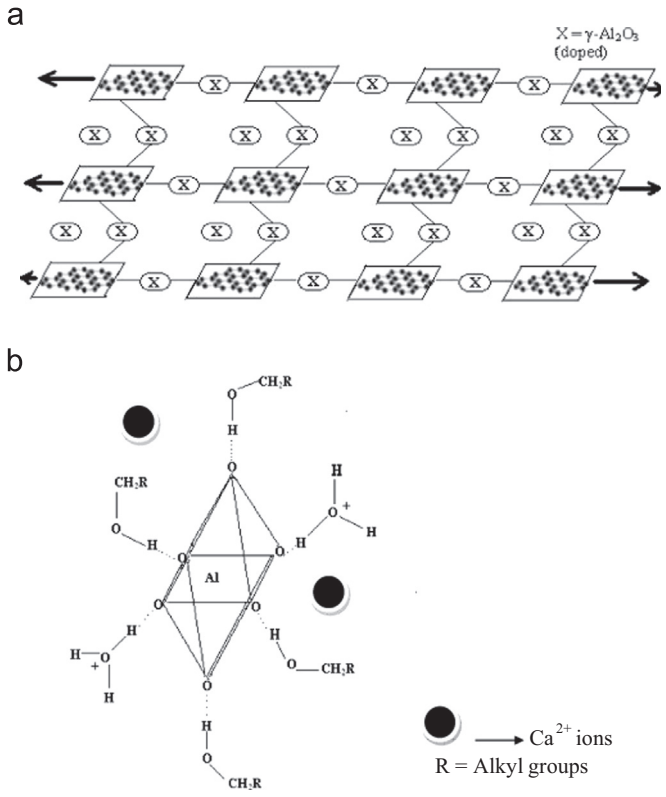

Fig. 4. (a) Bridging mechanism of exfoliated graphite platelets via intercalated doped γ-Al_2O_3 nanophases; (b) Schematic representation of growing moiety of γ-Al_2O_3.

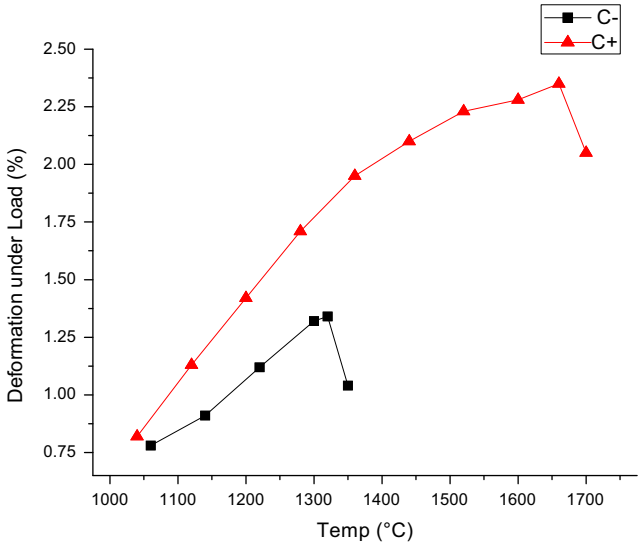

Fig. 5. Comparison of RUL plots of C+ and C− castables.

Fig. 5 shows the RUL plots of C+ and C− castables noted particularly beyond 1000 °C. C+ exhibits a remarkable increase in the RUL behavior (in terms of T_0 and T_a values) in comparison with C− castables. It is clearly observed that the subsidence of C− takes place beyond 1300 °C whereas in C+ it is far above 1600 °C. As the porosity of C− castable is significantly higher, it is difficult to collapse them by sintering. It is known that the resistance of refractory to flow under stress can be increased by increasing the proportion of crystalline materials. C+ and C− castables differ only in the characteristics of graphite besides possessing the same chemical and mineralogical composition. As the crystalline graphite in the C− matrix is practically unprotected it is more prone to oxidation in the furnace heating atmosphere. Oppositely the thin coating of calcium aluminate retained the crystalline graphites within the C+ matrix for a much prolonged period with significant increase in RUL values. It is also known that the castable deformation during RUL test takes place due to the sliding and flow of refractory grains surrounding the liquid phases like $CaO–Al_2O_3–SiO_2$ and/or $CaO–MgO–Al_2O_3–SiO_2$ [21]. If the solid to solid adhesion is stronger, by keeping the liquid in isolated pockets, the RUL property can be improved. C− castables already containing a lot of pores are unable to prevent the matrix-aggregate debonding. In contrast the matrix-aggregate bonding is more compatible in C+ castable having lesser porosity. The coating promotes intimate contact between aggregate and matrix, enhancing more densification and less deformation. It prevents the detachment between matrix and aggregate and controls the relative movement of grains in a better densified matrix. More importantly the formation and growth of hibonite crystals ($CaO.6Al_2O_3$) beyond 1350 °C enhances the interlocking bonding between spinel fines and rest part of C+ matrix; but as C− castables collapses earlier, CA_6 formation is not exploited in the inferior quality of C− matrix. For this reason the C.C.S values of C+ castables are much better than C− castables. It has been reported that nanoplatelets of graphene oxide sheets helped to arrest, bridge and deflect cracks efficiently in comparison with the untreated graphite [36]. The evolution of a toughened ceramic matrix is quite likely, in a similar manner, in C+ castable. This improved mechanical strength of partially exfoliated graphite must have played a significant role to improve the RUL property of C+ castable manifold. As the coated graphites are selectively cross linked with Ca^{2+} and Al^{3+} ions (Fig. 4), the mechanical stiffness and fracture strength of partially converted graphene oxide sheets increase remarkably [35]. It has been explained by Raman studies that due to the heat treatment and ultra-sonication employed during the coating formation over graphite, the graphite sheets are partially exfoliated and intercalated [24]. As such the Ca^{2+} and Al^{3+} ions from calcium doped γ-Al_2O_3 in functionalized graphite layers help in controlled clumping to withstand high pressure on C+ matrix with increasing temperature. Last but not the least, the reactive nanosheets of graphite also helped to develop the silicon carbide phases in the castable matrix even at elevated temperature [13]. The XRD plot of fired C+ matrix (Fig. 6**a**) shows that silicon carbide phases had been generated in the matrix. It can be due to the course of reactions between microsilica, reactive alumina and graphite as reported in literature [37]. Low thermal expansion, high thermal conductivity and high strength of moissanite/silicon carbide phases are appreciated for refractory applications. In addition, the reinforcing effect of SiC crystallites integrated into spinel-corundum castable matrix must significantly contribute to the RUL behavior [38]. These whiskers reinforce the matrix and tremendously improve the load bearing capacity of the composite refractory. All these render a combined effort for the enormous increase of RUL value for the respective castable.

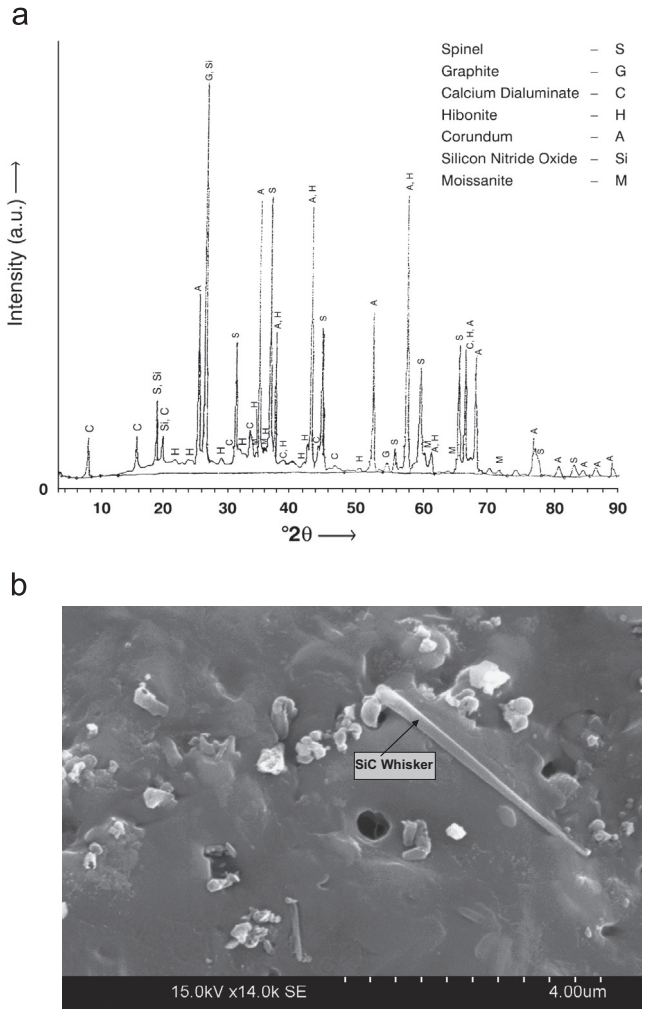

Fig. 6. (a) XRD plot of C+ matrix fired at 1500 °C; (b) SEM micrograph of C+ matrix fired at 1500 °C.

As the mechanical properties (e.g. tensile strength, compressibility) of graphite changes drastically with temperature [3], the exfoliation and subsequent intercalation of graphite sheets can bear with compressive load at increasing temperatures. As such, the improvement in RUL is more significant than the CCS properties of C+ castables.

XRD of C+ matrix (Fig. 6**a**) shows that besides the desired phases of corundum and calcium aluminate, the strong peak of graphite is prominently present in the matrix even after heat treatment at 1500 °C. Graphite has been retained obviously due to the calcium aluminate coating as explained before. The XRD plot indicates the evolution of two other phases namely silicon carbide (Moissanite) and silicon oxide nitride. This confirms that the antioxidising characteristics are maintained within the C+ matrix even after 1500 °C firing. As the matrix contains reactive microsilica, it is obvious that silicon carbide phases would prevail in carbon enriched matrix. The mechanism of SiC generation in CO(g) atmosphere at elevated temperature, by interaction of C and SiO_2, has been depicted in literature [37]. It has been assured that 0.1 mol of CO for almost 100 mol of solid refractory mass can provide a reducing atmosphere. That paper also outlined the preferential formation of CA_2 and CA_6 in presence of CO(g). Some other literatures show that in-situ formation of SiC_xO_y, Al_4C_3, Al_2OC, TiC, AlN and TiCN coatings in carbon containing refractories improve the oxidation resistance [8,27]. According to the XRD report, similar compounds had also been formed in the C+ refractory castable. Literature also shows that graphene oxide nanosheets can promote the formation of silicon carbide whiskers in the Al_2O_3–C refractory at high temperature [13]. It is due to the higher reactivity of graphene oxide nanosheets (GONs) than graphite flakes that yielded silicon oxycarbide fibers with high aspect ratio to strengthen the refractory. Such kind of long, thick and locally developed fibrous structures, rich in silicon and carbon [8], had also been observed in this work inside the matrix enriched with refractory oxides (Fig. 6b). Depending on the partial pressure of carbon monoxide, oxygen and nitrogen, the silicon oxide nitride had also been developed; it too helped in forming a highly compact composite matrix of C+ castable which contributed to superior mechanical properties. Formation of carbide and nitride phases in Al_2O_3–C and MgO–C refractories containing carbon nanotubes and graphite oxide nanosheets can render a positive influence on the thermomechanical properties [8,12]. We suggest that similar coatings of moissanite [**PDF:** 00–039-1196] and silicon oxynitride [**PDF:** 01–079-1539] phases (Fig. 6a) had remarkably improved the oxidation resistance of C+ castables as shown in (Fig. 7). Silicon oxynitride (Si_2N_2O) also exhibits superior oxidation resistance to that of SiC and Si_3N_4 and possesses good mechanical properties [39]. Formation of silicon oxynitride phases, however, needs further clarification. Heating silica and carbon in controlled N_2 atmosphere at high temperature can promote its formation. It is reported that furnace atmosphere with increasing p_{N2} can assist formation of oxynitride phases from SiO(g) [40]. As microsilica was present in castable batch, local change of furnace atmosphere thus resulted in small amount of Si_2N_2O crystallites. Yamaguchi identified the stable areas of condensed species (e.g. nitrides) in the systems Si–C–N–O, Al–Si–C–O, Si–C–O and Al–C–N–O etc. for changing partial pressures of N_2(g) and CO(g) [41]. Literature also suggests formation of trace amount of Si_2N_2O at ~1500 °C with SiC by carbothermic reduction of SiO_2 to SiO(g) and CO(g). The reaction rate was strongly dependent upon (C/SiO_2) mole ratio, specific surface area and particle size distribution of SiO_2 and C (graphite) [42]. Small amount of oxynitride formation via multistage thermodynamic mechanisms had been described during combustion in air in presence of γ-Al_2O_3 nanopowders [43]. It can be thus safely advocated that feeble amount of Si_2N_2O has been crystallized which also deoxidizes CO(g) to C(s) improving the sustainability of surface-modified graphites.

The photographs of C+ and C− cylinders after oxidation resistance test are displayed in Fig. 7. The presence of more intense black zone is very much conspicuous in C+ cylinder after oxidation test. The distribution of graphite is noticeably less in C− both in diametric and axial directions. [8,27]. As both C+ and C− were embedded in carbon bed, it can be considered that CO(g) must be present to slow down the

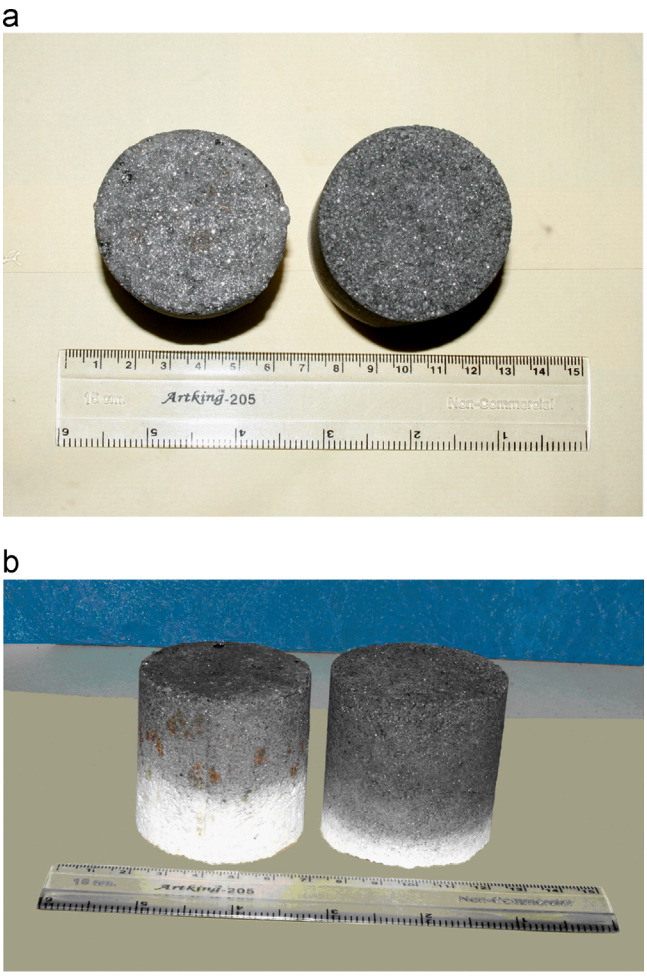

Fig. 7. (a and b): Photographs of C+ (right) and C− (left) castables after oxidation resistance test.

oxidation of castable constituents. Still the carbon-depleted region was visibly quite large in C− in comparison with the other. Oxidation depth at several positions had also been measured and C+ excelled once again. Nanostructured thin Ca-doped γ-Al_2O_3 coating thus minimized the CO(g) emission to additionally assure pollution control up to a reasonable extent.

4. Conclusions

Sustaining graphite in the castable system for a longer period had been seriously attempted by refractory scientists. However, the commercial potential towards the utilization of the calcium–aluminate coated graphite in steel plants has not yet been given any attention. In order to fill this knowledge gap, an attempt has therefore, been made in the present work to utilize the coated graphite in unshaped refractories. This laboratory scale investigation gave a strong indication on the enormous improvement of refractory properties of alumina–carbon castables containing 5.0% of coated graphite. Refractoriness under load and oxidation resistance had been satisfactorily upgraded. Nanostructured calcium aluminate coating, partial exfoliation and intermittent clumping of functionalized graphite sheets had been identified to be the key factors for this performance. Microstructural aspects and phase evolution studies confirmed that, along with the evolution of other desirable phases, graphite has been retained well in the refractory matrix after aggressive heat treatment.

Acknowledgments

The authors thankfully acknowledge Prof. T.K. Parya and Dr. P.K. Maiti of Department of Chemical Technology, Calcutta University, for their help extended during the course of this investigation.

References

[1] S. Zhang, Next generation carbon containing refractory composites, Advances in Science and Technology, vol-45, Trans Tech Publications, Switzerland2246–2253.
[2] M. Nouri-Khezrabad, M.A.L Braulio, V.C. Pandolfelli, F. Golestani-Fard, H.R. Rezaie, Nano-bonded refractory castables, Ceramics International 39 (4) (2013) 3479–3497.
[3] EMM Ewais, Carbon based refractories, Journal of the Ceramic Society of Japan 112 (1310) (2004) 517–532.
[4] M. Bag, S. Adak, R. Sarkar, Study on low carbon containing MgO–C refractory: use of nano carbon, Ceramics International 38 (3) (2012) 2339–2346.
[5] X. Liu, S. Zhang, Low-temperature preparation of titanium carbide coatings on graphite flakes from molten salts, Journal of the American Ceramic Society 91 (2008) 667–670.
[6] S. Mukhopadhyay, S. Dutta, Sk.A. Ansar, S. Das, S. Misra, Spinel-coated graphite for carbon containing refractory castables, Journal of the American Ceramic Society 92 (8) (2009) 1895–1900.
[7] S. Dutta, P. Das, A. Das, S. Modak, S. Mukhopadhyay, Physical characteristics of alumina–carbon refractory castables containing calcium aluminate-coated graphites, Interceram-Refractories Manual 62 [4] (2013).
[8] M. Luo, et al., Microstructure and mechanical properties of multi-walled carbon nanotubes containing Al_2O_3–C refractories with addition of polycarbosilane, Ceramics International 39 (2013) 4831–4838.
[9] V. Roungos, C.G. Aneziris, Improved thermal shock performance of Al_2O_3–C refractories due to nanoscaled additives, Ceramics International 38 (2012) 919–927.
[10] Y. Klemm, H. Biermann, C.G. Aneziris, Microstructure and mechanical properties of fine grained carbon-bonded Al_2O_3–C materials, Ceramics International 39 (2013) 6695–6702.
[11] J. Liu, H. Yan, K. Jiang, Mechanical properties of graphene platelet-reinforced alumina ceramic composites, Ceramics International 39 (2013) 6215–6221.
[12] T. Zhu, et al., Microstructure and mechanical properties of MgO–C refractories containing graphite oxide nanosheets (GONs), Ceramics International 39 (3) (2013) 3017–3025.
[13] Q..Wang,Y..Li, M..Luo, S..Sang, T..Zhu, L..Zhao, Strengthening mechanism of graphene oxide nanosheets for Al_2O_3–C refractories, Ceramics International, http://dx.doi.org/10.1016/j.ceramint.2013.05.117.
[14] K. Kawabata, H. Yoshimatsu, E. Fuji, K. Hiragushi, A. Osaka, Properties of Al_2O_3–C castable refractories with graphite powder coated with alumina, Journal of the Ceramic Society of Japan 109 (2001) 270–273.
[15] S. Yilmaz, Y. Kutmen-Kalpakli, E. Yilmaz, Synthesis and characterization of boehmitic alumina coated graphite by sol–gel method, Ceramics International 35 (2009) 2029.
[16] J. Ye, R.P. Thackray, W.E. Lee, S. Zhang, Microstructure and rheological properties of titanium carbide-coated carbon black particles synthesized from molten salt, Journal of Materials Science 48 (2013) 6269–6275.
[17] S. Zhang, W.E. Lee, Improving the water-wettability and oxidation resistance of graphite using Al_2O_3/SiO_2 sol–gel coatings, Journal of the European Ceramic Society 23 (2003) 1215–1221.

[18] S. Mukhopadhyay, Improved sol gel spinel ($MgAl_2O_4$) coatings on graphite for application in carbon containing high alumina castables, Journal of Sol–Gel Science and Technology 56 (1) (2010) 66–74.
[19] A. Saberi, F. Golestani-Fard, M.W. Porada, R. Simon, T. Gardes, H. Sarpoolaky, Improving the quality of nanocrystalline $MgAl_2O_4$ spinel coating on graphite by a prior oxidation treatment on the graphite surface, Journal of the European Ceramic Society 28 (10) (2008) 2011–2017.
[20] Sk.A. Ansar, S. Bhattacharya, S. Dutta, S.S. Ghosh, S. Mukhopadhyay, Development of mullite and spinel coatings on graphite for improved water-wettability and oxidation resistance, Ceramics International 36 (6) (2010) 1837–1844.
[21] S Mukhopadhyay, Sk.A. Ansar, D Paul, G Bhowmick, S. Sengupta, Characteristics of refractory castables containing mullite and spinel coated graphites, Materials and Manufacturing Processes 27 (2) (2012) 177–184.
[22] S. Mukhopadhyay, G. Das, I. Biswas, Nanostructured cementitious sol–gel coating on graphite for application in monolithic refractory composites, Ceramics international 38 (2) (2012) 1717–1724.
[23] S. Mukhopadhyay, S. Dutta, Comparison of solid state and sol–gel derived calcium aluminate coated graphite and characterization of prepared refractory composite, Ceramics International 38 (6) (2012) 4997–5006.
[24] S. Mukhopadhyay, Nanoscale calcium aluminate coated graphite for improved performance of alumina based monolithic refractory composite, Materials Research Bulletin 48 (7) (2013) 2583–2588.
[25] A.K. Bhattacharya, P. Bandopadhyay, Study on the physicochemical behavior of graphite of eastern India—used for refractory manufacture, Refractories Manual (Interceram: Special Edition) (2009) 36–40.
[26] H. Yoshimatsu, et al., Wettability by water and oxidation resistance of alumina-coated graphite powder, Journal of the Ceramic Society Japan 103 (9) (1995) 929–934.
[27] C.G. Aneziris, J. Hubalkova, R. Barabas, Microstructure evaluation of MgO–C refractories with TiO_2 and Al additions, Journal of the European Ceramic Society 27 (2007) 73–78.
[28] S. Pei, H.M. Cheng, The reduction of graphene oxide, Carbon 50 (9) (2012) 3210–3228.
[29] R. Schlogl, Graphite: A Unique Host Lattice, Kluwer Academic Publishers; Netherlands, 1994, pp 83–176.
[30] W. Zhao, P.H. Tan, J. Liu, A.C. Ferrari, Intercalation of few-layer graphite flakes with $FeCl_3$: Raman determination of fermi level, layer by layer decoupling, and stability, Journal of the American Chemical Society 133 (2011) 5941–5946.
[31] A. Banerjee, S. Das, S. Misra, S. Mukhopadhyay, Structural analysis of spinel ($MgAl_2O_4$) for application in spinel-bonded castables, Ceramics International 35 (2009) 381–390.
[32] M. Pijolat, et al., Influence of water vapour and additives on the surface area stability of γ-Al_2O_3, Solid State Ionics 50 (1992) 31–39.
[33] S. Chen, Z. Zhu, X. Wu, Q. Han, X. Wang, Graphene oxide–MnO_2 nanocomposites for supercapacitors, ACS Nano 4 (5) (2010) 2822–2830.
[34] S. Soled, γ-Al_2O_3 viewed as a defect oxyhydroxide, Journal of Catalysis 81 (1) (1983) 252–257.
[35] S. Park, K-Seok lee, G. Bozoklu, W. Cai, S.T. Nguyen, R.S. Ruoff, Graphene oxide papers modified by divalent ions—enhancing mechanical properties via chemical cross-linking, ACS Nano 2 (3) (2008) 572–578.
[36] L.S. Walker, V.R. Marotto, M.A. Rafiee, N. Koratkar, E.L. corral, Toughening in graphene ceramic composites, ACS Nano 5 (4) (2011) 3182–3190.
[37] A.P. Luz, V.C. Pandolfelli, Thermodynamic evaluation of SiC oxidation in Al_2O_3–$MgAl_2O_4$–SiC–C refractory castables, Ceramics International 36 (6) (2010) 1863–1869.
[38] F. Ye, M. Rigaud, X. Liu, X. Zhong, High temperature mechanical properties of bauxite-based SiC-containing castables, Ceramics International 30 (2004) 801–805.
[39] Y. Miyamoto, S. Kanehira, M. Radwan, Recycling of industrial and natural wastes to SiAlONs, Refractories Applications and News 9 (1) (2004) 14–17.
[40] T. Das, Oxynitride glasses—an overview, Bulletin of Material Science 23 (6) (2000) 499–507.
[41] A. Yamaguchi, Application of thermochemistry to refractories, in fundamentals of refractory technology, in: J.P. Bennett, J.D. Smith (Eds.), Ceramic Transactions, 125, The American Ceramic Society, OH 43081, USA, 2001, pp. 157–170.
[42] J.P. Murray, A. Steinfeld, E.A. Fletcher, Metals, nitrides and carbides via solar carbothermal reduction of metal oxides, Energy 20 (7) (1995) 695–704.
[43] A.A. Gromov, E.M. Popenko, A.V. Sergienko, A.P. Il′in, V. I Vereshchagin, Nitride formation during combustion of ultrafine aluminum powders in air. I. Effect of additives, Combustion, Explosion and Shock Waves 41 (3) (2005) 303–314.